

# Fermionic Superradiance in a Transversely Pumped Optical Cavity

J. Keeling,<sup>1</sup> M. J. Bhaseen,<sup>2</sup> and B. D. Simons<sup>3</sup>

<sup>1</sup>*SUPA, School of Physics and Astronomy, University of St Andrews, St Andrews KY16 9SS, United Kingdom*

<sup>2</sup>*Department of Physics, King's College London, Strand, London WC2R 2LS, United Kingdom*

<sup>3</sup>*University of Cambridge, Cavendish Laboratory, Cambridge CB3 0HE, United Kingdom*

(Dated: September 27, 2018)

Following the experimental realization of Dicke superradiance in Bose gases coupled to cavity light fields, we investigate the behavior of ultra cold fermions in a transversely pumped cavity. We focus on the equilibrium phase diagram of spinless fermions coupled to a single cavity mode and establish a zero temperature transition to a superradiant state. In contrast to the bosonic case, Pauli blocking leads to lattice commensuration effects that influence self-organization in the cavity light field. This includes a sequence of discontinuous transitions with increasing atomic density and tricritical superradiance. We discuss the implications for experiment.

PACS numbers: 37.30.+i, 42.50.Pq

*Introduction.*— Experiments combining cold atomic gases with cavity quantum electrodynamics (QED) have led to pivotal developments in matter-light interaction. The use of Bose–Einstein condensates (BECs) allows precise control over the collective matter-light coupling, and permits access to the strong coupling regime [1, 2]. This may be exploited for spectroscopy of many body systems [3–5], and to induce light-mediated interactions.

Early theoretical work predicted that atoms in a cavity undergo a self-organization transition when pumped transversely [6–8]. This was confirmed by experiments on thermal clouds and recently on a BEC [9–11]. The latter also established equivalence to the superradiance transition in an effective Dicke model [12–17]. These advances open the door to non-equilibrium and strongly correlated matter-light phenomena, including driven-dissipative phase transitions [18, 19], Mott insulator transitions in self-organized lattices [20, 21] and cavity optomechanics [22]. They also provide a platform on which to explore frustrated spin models and glassy behavior in multimode cavities [23–27]. For a review see [28].

The experimental realization of superradiance in BECs raises many questions regarding the possible behavior of fermions in cavities. Recent investigations have considered longitudinal pumping [29, 30], cavity mediated pairing [31] and synthetic gauge fields [32]. In this manuscript we focus on the closest extension of recent experiments [10, 11] by coupling spinless fermions to a single mode of a transversely pumped cavity. At high temperatures, where both fermions and bosons exhibit Maxwell–Boltzmann statistics, it is evident that fermions will exhibit a superradiance transition, as observed for thermal bosons [9]. However, at low temperatures the Bose and Fermi gases are expected to behave differently and numerous questions arise. Does the self-organization transition survive for degenerate fermions? How does commensurability between the Fermi wavevector and the self-consistent optical lattice affect self-organization? Do new phases exist, and what characterizes the transitions?

*The Model.*— Inspired by Refs. [9–11], we consider spinless fermions coupled to a single mode of a cavity light field (forming a standing wave in the  $x$ -direction), and pumped by a transverse laser (in the  $z$ -direction); see inset of Fig. 1. We assume that the pump frequency  $\omega_p$

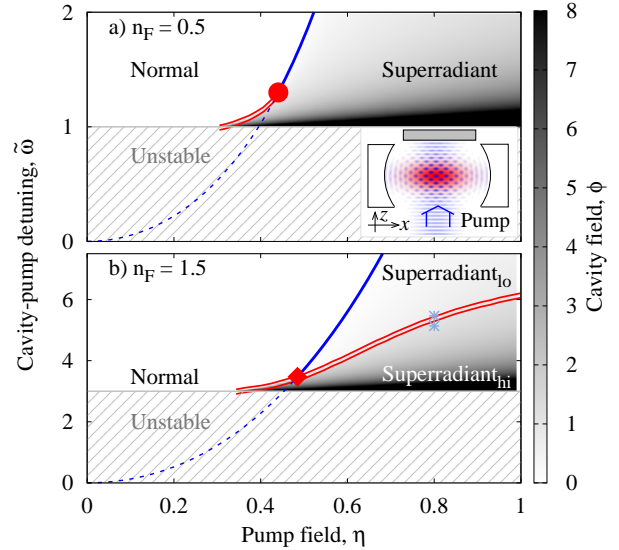


FIG. 1. Equilibrium phase diagram of fermions in a transversely pumped cavity; see inset. As the pumping is increased there is a transition to a superradiant (SR) state, where the fermions spontaneously “self-organize” in the self-consistent light field. The panels correspond to partial filling of (a) the first and (b) second bands of the emergent lattice. At large detuning the cavity field (grayscale) grows continuously above a critical pump field (solid blue line), whilst at smaller detuning the transition is discontinuous (double red line). These first and second order boundaries join differently at different fillings; for  $n_F \lesssim 1$  they meet at a tricritical point (circle) whilst at higher fillings there is a critical endpoint (diamond). The first order boundary in (b) corresponds to a liquid-gas type transition within the SR phase. The unstable region  $\tilde{\omega} < 2n_F$  will be stabilized by cavity loss; see text. The dashed line is the spinodal extension of the continuous line.

is far detuned from the atomic transition frequency  $\omega_a$  so that absorption and consequent heating via spontaneous emission can be neglected. After eliminating the excited states of the atoms (see e.g. [33]), one obtains an effective Hamiltonian governing the interaction between the cavity light field and the motional degrees of freedom:

$$\hat{H} = \hbar\omega\hat{\psi}^\dagger\hat{\psi} + \sum_{\mathbf{k}} \left[ \frac{\hbar^2 k^2}{2m} \hat{c}_{\mathbf{k}}^\dagger \hat{c}_{\mathbf{k}} - \frac{g^2}{4\Delta_a} \hat{\psi}^\dagger \hat{\psi} \sum_s \hat{c}_{\mathbf{k}}^\dagger \hat{c}_{\mathbf{k}+2s\mathbf{q}_x} - \frac{g\Omega}{4\Delta_a} (\hat{\psi} + \hat{\psi}^\dagger) \sum_{s,s'} \hat{c}_{\mathbf{k}}^\dagger \hat{c}_{\mathbf{k}+s\mathbf{q}_z+s'\mathbf{q}_x} - \frac{\Omega^2}{4\Delta_a} \sum_s \hat{c}_{\mathbf{k}}^\dagger \hat{c}_{\mathbf{k}+2s\mathbf{q}_z} \right] \quad (1)$$

where  $\Delta_a \equiv \omega_a - \omega_p$  and  $s, s' \in \pm 1$  denotes the forward and backward components of the standing waves. Here,  $\hat{c}_{\mathbf{k}}$  is an annihilation operator for a spinless fermion with mass  $m$  and wavevector  $\mathbf{k}$ , and  $\hat{\psi}$  is a bosonic annihilation operator for cavity photons. Eq. (1) is written in the rotating frame of the pump so  $\omega \equiv \omega_c - \omega_p$  is the cavity-pump detuning. To ensure efficient scattering between the pump and the cavity, the cavity frequency  $\omega_c$  is assumed to be close to  $\omega_p$ . The cavity and pump light fields thus have approximately equal wavelengths with  $|\mathbf{q}_x| = |\mathbf{q}_z| = q$ . Scattering between the pump and the cavity involves the cavity-atom coupling  $g$ , and the pump strength  $\Omega$ , and is described by the fourth term in Eq. (1). The third (fifth) term corresponds to a second order process involving the absorption and emission of cavity (pump) photons. For bosons, there are limits where one may truncate the number of  $\mathbf{k}$ -states; when truncated to  $\mathbf{k} = (0, 0)$  and  $\mathbf{k} \in (\pm q, \pm q)$ , the Hamiltonian maps on to an effective Dicke model describing two-level systems coupled to light [10, 16, 17, 33]. For fermions, Pauli blocking generally precludes truncation and so we must consider the higher  $\mathbf{k}$ -states.

In a “self-organized” state, the cavity light field develops an expectation  $\langle \hat{\psi} \rangle \neq 0$ , and the superposition of the pump and cavity fields forms a 2D lattice with reciprocal lattice vector  $(q, q)$ . We introduce dimensionless units by measuring atomic energies in units of the recoil energy  $E_R \equiv \hbar^2 q^2 / 2m$ . Wavevectors (and lengths) are measured in units of the magnitude of the reciprocal lattice vector  $\sqrt{2}q$  so that the resulting Brillouin Zone (BZ) has unit area. We consider atoms confined to a 2D layer in the  $x, z$  plane and thus define the filling fraction  $n_F \equiv N/N_l$  as the number of atoms per lattice site;  $N_l = 2q^2 \mathcal{A} / (2\pi)^2$  for a real space area  $\mathcal{A}$ . From Eq. (1) it is natural to introduce dimensionless pump and cavity fields via  $\eta^2 = \Omega^2 / 4\Delta_a E_R$  and  $\phi^2 = g^2 \langle \hat{\psi} \rangle^2 / 4\Delta_a E_R$ .

*Equilibrium Phase Diagram.*— We begin by determining the equilibrium phase diagram for the Hamiltonian (1). Although this neglects cavity losses, key features will survive in this limit [10, 11]. We treat the cavity mode in mean-field theory, which is exact in the thermodynamic

limit  $N, \mathcal{A} \rightarrow \infty$  [34]. Considering the dimensionless free energy density  $f = F / (E_R N_l)$ , we find:

$$f = \tilde{\omega} |\phi|^2 - \tilde{\beta}^{-1} \int_{BZ} d^2 k \sum_n \ln \left[ 1 + e^{-\tilde{\beta}(\epsilon_{\mathbf{k},n} - \mu)} \right] + \mu n_F, \quad (2)$$

where  $\tilde{\omega} \equiv \omega(4\Delta_a/g^2 N_l)$  is a dimensionless cavity-pump detuning. Here,  $\epsilon_{\mathbf{k},n}$  is the energy in the  $n$ th band, found by diagonalizing the atomic part of Eq. (1). Both  $\epsilon_{\mathbf{k},n}$  and  $\mu$  are in units of  $E_R$ , and  $\tilde{\beta} \equiv E_R/k_B T$ . To ensure that  $\mu$  is unambiguously defined, even for filled bands, we work at a low non-zero temperature,  $k_B T = 0.05 E_R$ , throughout. Minimization of  $f$  at fixed  $n_F$  yields Fig. 1.

Figure 1 shows two fillings, characteristic of a partially filled first band (panel a,  $n_F = 0.5$ ) and a partially filled second band (panel b,  $n_F = 1.5$ ). In both cases, two phases exist. At low  $\eta$  there is a normal state with  $\phi = 0$ . At large  $\eta$ ,  $\phi \neq 0$  and this state is labelled “superradiant” (SR) by analogy with the Dicke model terminology [13–17]. It is also “self-organized” as the fermions are arranged in a self-consistent optical lattice.

*Landau Theory.*— As found in the bosonic case [10, 11], the normal-SR transition is second order at high  $\eta$  and  $\tilde{\omega}$ . However, for the partially filled first band, on decreasing  $\eta$ , a tricritical point occurs beyond which the transition becomes first order. This can be understood via a Landau expansion,  $f = f_0 + a(\tilde{\omega}, \eta, n_F)\phi^2 + b(\eta, n_F)\phi^4 + c(\eta, n_F)\phi^6$ , where pump-cavity phase-locking ensures  $\phi \in \mathbb{R}$ . Taking  $c > 0$  for stability, three types of behavior occur depending on the sign of  $b$  [35]. For  $b > 0$  a continuous transition occurs at  $a = 0$ , whilst a first order transition occurs at  $a = b^2/4c$  when  $b < 0$ . These transitions meet at a tricritical point at  $a = b = 0$ . In the vicinity of the tricritical point the critical exponent describing the onset of the cavity field  $\phi$  changes from  $\beta = 1/2$  to  $\beta = 1/4$ . At low  $\eta$ ,  $b(\eta, n_F) < 0$  and so the boundary becomes first order in Fig. 1 (a).

The physical origin of this discontinuous transition is reminiscent of the Larkin–Pikin mechanism [36], where coupling to an additional degree of freedom drives a transition first order. Here, the order parameter  $\phi$  couples to density waves of the atomic system. The linear coupling to the  $\cos(x/\sqrt{2})\cos(z/\sqrt{2})$  density wave described by the fourth term in Eq. (1) yields a continuous transition. However, the quadratic coupling to the  $\cos(\sqrt{2}x)$  density wave in the third term in Eq. (1) drives  $b < 0$  at small  $\eta$ , as follows from second order perturbation theory. Note that this mechanism is distinct from the Brazovskii scenario for driving the self-organization transition first order in multimode cavities [23, 24].

The behavior described so far persists while only the first band is filled. Richer behavior occurs when higher bands start to be filled; see Fig. 1 (b). Here, there is no tricritical point and the second order line terminates at a critical endpoint [35]. The SR phase is now divided by a first order transition, separating high and low  $\phi$

regions. This is analogous to a liquid-gas transition, and the two phases are connected by a trajectory at lower  $n_F$ . Within Landau theory this corresponds to terms beyond  $\phi^4$  being negative. We will return to the physical origin of this transition later in the manuscript.

*Unstable Regions.*— As indicated in Fig. 1, when  $\tilde{\omega} < 2n_F$ ,  $f$  is unbounded from below. This reflects the form of  $f$  at large  $\phi$ , when the atoms are trapped in deep minima of the cavity optical lattice. Here, the leading contribution to the atomic energy is  $\epsilon_{\mathbf{k},n} \sim -2\phi^2$  and so  $f \sim (\tilde{\omega} - 2n_F)\phi^2$ . The unstable region exists even at low densities, where Pauli blocking can be ignored, and so it is also relevant for bosons. Such a situation has been discussed for bosons in Ref. [37]. However, as we argued in Ref. [33], this instability will be replaced by dynamical attractors in the presence of cavity losses.

*Continuous Phase Boundaries.*— Where the boundaries are continuous, the  $\eta, n_F$  dependence of the critical detuning  $\tilde{\omega}$  can be obtained from the vanishing quadratic Landau coefficient. This has contributions from the first and third terms in Eq. (1). Using second order perturbation theory,  $a(\tilde{\omega}, \eta, n_F) = \tilde{\omega} + \chi(\eta, n_F)$ , where

$$\chi(\eta, n_F) = 2\eta^2 \int_{BZ} d^2k \sum_{ij} n_F(\epsilon_{\mathbf{k},i}) \frac{|\langle u_{\mathbf{k},i} | \hat{M} | u_{\mathbf{k},j} \rangle|^2}{\epsilon_{\mathbf{k},i} - \epsilon_{\mathbf{k},j}}, \quad (3)$$

is a dimensionless atomic susceptibility. Here,  $\epsilon_{\mathbf{k},i}$  and  $|u_{\mathbf{k},i}\rangle$  are the atomic energies and eigenstates evaluated in the absence of the cavity field. The pump-cavity scattering represented by the third term in Eq. (1) corresponds to  $\hat{M} = 4 \cos(x/\sqrt{2}) \cos(z/\sqrt{2})$  in the position basis. At  $\phi = 0$  the wavefunctions  $\langle x, z | u_{\mathbf{k},i} \rangle$  factorize into plane-waves in the  $x$  (cavity) direction and Mathieu functions [38] in the  $z$  (pump) direction due to the pump lattice. The phase boundary occurs at  $\tilde{\omega} = -\chi$ ; for parameters where the boundary turns first order, this becomes the spinodal line [35] as shown by the dashed lines in Fig. 1.

In the limits of low and high pump field, analytical results for the boundaries may be obtained. For  $\eta \rightarrow 0$  the Mathieu functions are plane waves and one finds  $\chi = -4\pi\eta^2(1 - \Theta(\gamma)\sqrt{|\gamma|})$  where  $\Theta(\gamma)$  is a Heaviside step function and  $\gamma = 1 - 4n_F/\pi$ . The sharp threshold reflects Pauli blocking: at high densities the susceptibility saturates due to states deep within the Fermi surface (FS) not contributing. The threshold occurs when  $n_F = \pi k_F^2 = \pi/4$  or  $2k_F = 1$ . i.e. when the FS diameter matches the scattering wavevector represented by the third term in Eq. (1). Note however that at low  $\eta$  the phase boundary is actually first order, so  $\tilde{\omega} = -\chi$  is a spinodal line. The  $\eta^2$  dependence is evident from the dashed line in Fig. 1. In the low density and low pump field limit this corresponds to  $\tilde{\omega} = 8\eta^2 n_F$ , which is where the Dicke approximation would erroneously predict a transition. As  $\eta \rightarrow \infty$ , the Mathieu functions are very localized so the dispersion in  $k_z$  is flat, while remaining quadratic in  $k_x$ . The bands induced by the

pump are well separated and so only the lowest band need be considered, yielding  $\chi = 16\eta^2 \ln|(1 - n_F)/(1 + n_F)|$ . The divergence at  $n_F = 1$  is a consequence of FS nesting. For a flat  $z$  dispersion the FS is delimited by  $|k_z| < 1/\sqrt{2}$ ,  $|k_x| < n_F/2\sqrt{2}$ , and the cavity-pump scattering induces atomic scattering,  $k_x \rightarrow k_x \pm 1/\sqrt{2}$  at a nesting wavevector for  $n_F = 1$ . At finite  $\eta$  the logarithmic singularity is softened by imperfect nesting but a peak remains unless  $\eta \ll 1$ ; we will return to this below.

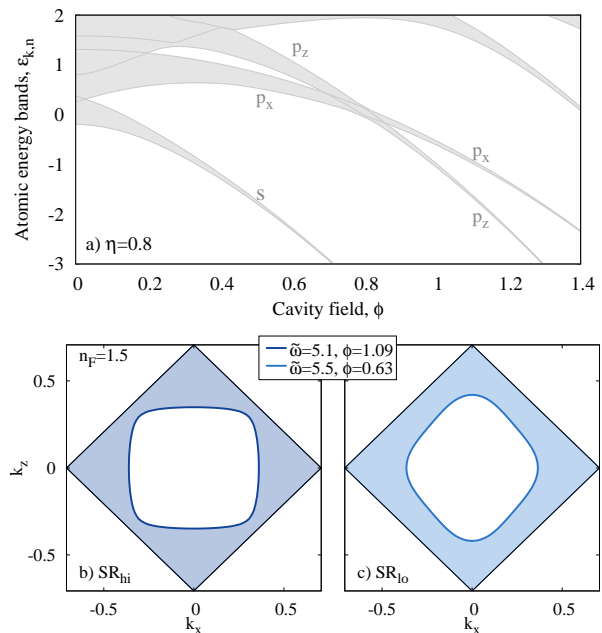


FIG. 2. (a) Atomic bands versus  $\phi$  for  $\eta = 0.8$ . When filling the 2nd or higher bands,  $f(\phi)$  is non-monotonic, thus allowing first order liquid-gas type transitions in the SR phase. (b) and (c) illustrate a distortion of the FS on crossing the liquid-gas boundary; the values of  $\tilde{\omega}$  are indicated by crosses in Fig. 1 (b). The FS delimits a partially filled second band and is shown in a reduced zone scheme. Occupied states are shaded.

*Liquid-Gas Transition.*— As noted earlier, for partial filling of the second (or higher) bands, a liquid-gas type transition exists. The origin of this transition is revealed by the dispersion of the self-consistent bands with cavity field  $\phi$ , as shown in Fig. 2 (a). There is a clear crossing of the  $p_x$ - and  $p_z$ -like bands when  $\phi \simeq \eta$ ; the bands are labelled by the symmetry of the Wannier orbitals at large  $\phi$ . This crossing leads to a kink in the atomic free energy at  $\phi \simeq \eta$ , and a maximum in  $f(\phi)$  separating two minima. This yields a discontinuous jump from a high field state ( $SR_{hi}$ ) with  $\phi \gtrsim \eta$  to a low-field state ( $SR_{lo}$ ) with  $\phi \lesssim \eta$ , accompanied by a distortion of the FS; see Figs. 2 (b) and (c). More generally, the dispersion of the higher bands is non-monotonic in  $\phi$  and further band crossings can occur. Filling such bands leads to a non-monotonic  $f(\phi)$ , and hence additional liquid-gas type transitions.

*Evolution with Filling.*— Further insight into the

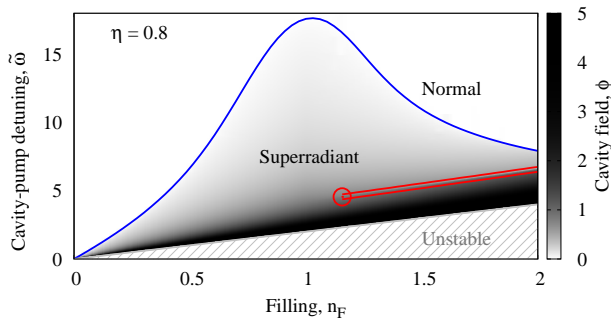


FIG. 3. Equilibrium phase diagram as a function of  $n_F$  at  $\eta = 0.8$ . The lines and the grays are as in Fig. 1. A critical point (empty circle) terminates the liquid-gas like transition at  $n_F \gtrsim 1$ . The second order normal-SR transition shows a peak near  $n_F \simeq 1$  reflecting nesting; see text.

liquid-gas transition is obtained from the phase diagram as a function of  $n_F$  at fixed  $\eta$ ; see Fig. 3. There is a critical point within the SR phase for  $n_F \gtrsim 1$ , beyond which a liquid-gas boundary extends. This corresponds to the point at which a sufficient fraction of the 2nd band is filled in order to introduce the required local minima in  $f(\phi)$ . Also visible in Fig. 3 is a peak in the second order boundary  $\tilde{\omega} = -\chi$  near  $n_F = 1$ . As  $\eta$  increases, this evolves into the logarithmic singularity of  $\chi$  at  $n_F = 1$ , reflecting the FS nesting discussed above.

*Non-Equilibrium, Linear Stability.*— Thus far we have provided a detailed analysis of the equilibrium properties of Eq. (1). However, as discussed in Refs. [33, 39], a finite cavity decay rate  $\kappa$  can significantly change the phase diagram. In a driven-open system, the phase diagram is found by determining the stable attractors of the dynamics, not by minimizing the free energy. Nonetheless, extrema of  $f$  correspond to stationary points of the dynamics in the limit  $\kappa \rightarrow 0$ . The open system thus inherits key features from its equilibrium counterpart [10, 11]. We next discuss which features are robust to non-zero  $\kappa$ , and which aspects require further investigation.

A feature that will survive when  $\kappa \neq 0$  is the boundary at which the normal state becomes unstable. This can be calculated by finding when the normal mode frequencies have negative imaginary parts [40]. Following the approach used for the bosonic system [16, 33] the boundary of stability is given by  $(\tilde{\kappa}^2 + \tilde{\omega}^2)/\tilde{\omega} = -\chi$ , where  $\chi$  is the atomic susceptibility given by Eq. (3) and  $\tilde{\kappa} \equiv 4\kappa\Delta_a/g^2N_l$ . In the limit  $\kappa \rightarrow 0$  one recovers the equilibrium result  $\tilde{\omega} = -\chi$  discussed above. This provides a direct link between the equilibrium and non-equilibrium phase boundaries, as found for the open Dicke model [10, 16, 17]. Unfortunately, a quantitative discussion of the fate of the first order boundaries is more challenging in the open fermionic system. Nonetheless, the existence of competing local minima in the equilib-

rium phase diagram suggests that multiple dynamical attractors may survive in the open limit. Likewise, determining the fate of the unstable region when  $\kappa \neq 0$  is difficult because it hinges on the long time dynamics of the fermionic system. This could potentially involve limit cycles, fixed points and chaotic attractors [40]. Indeed, the answer to the analogous question in the Dicke model [33] demonstrates both superradiant phases and limit cycles. It would be interesting to explore this in more detail, both theoretically and experimentally.

*Low Density Limit.*— As noted above, at low pump field, the normal-SR boundary always becomes first order, even as  $n_F \rightarrow 0$ . At low densities, the integral in Eq. (2) simplifies, and one finds that  $b(\eta, n_F)/n_F \rightarrow -1/2 + \mathcal{O}(\eta^2)$ . In this low density limit,  $k_F \ll q$ , this fermionic result also applies to bosons. Notably, this first order transition is absent from previous studies of bosons in single mode cavities. In particular, this discontinuous transition is lost when momentum states are truncated to yield the effective Dicke model [10, 16, 17, 33]; the transition involves hybridization with states  $(\pm 2q, 0)$  outside this basis. In the cases where higher momentum states have been considered [33, 41], this first order behavior was not captured due to focusing on the susceptibility and second order boundaries.

*Conclusions.*— We have explored the phase diagram of ultra cold fermions in a transversely pumped cavity. In contrast to a BEC, the interplay of the Fermi wavevector with the wavelength of the cavity field leads to a rich dependence on the filling fraction. We have established distinct superradiance transitions whose character reflects the impact of Pauli blocking and lattice commensuration. Unlike the Dicke model, the phase boundary turns first order at low pump field. In addition to signatures in the cavity light field, the measurable consequences include FS distortions and an enhanced susceptibility near unit filling. This study provides a basis for future experimental and theoretical research including the nature of dynamical attractors in the driven-dissipative system, the impact of fermion interactions, and the behavior in multimode geometries.

*Acknowledgments.*— We thank T. Esslinger for discussions and B. L. Lev for helpful comments on the manuscript. MJB and BDS acknowledge EPSRC EP/J017639/1 and MJB thanks the Thomas Young Centre. JK acknowledges support from EPSRC programme “TOPNES” (EP/I031014/1), EPSRC (EP/G004714/2), and hospitality from KITP Santa Barbara. This research was supported in part by the National Science Foundation under Grant No. NSF PHY11-25915.

---

[1] F. Brennecke, T. Donner, S. Ritter, T. Bourdel, M. Köhl, and T. Esslinger, *Nature* **450**, 268 (2007).

- [2] Y. Colombe, T. Steinmetz, G. Dubois, F. Linke, D. Hunger, and J. Reichel, *Nature* **450**, 272 (2007).
- [3] I. B. Mekhov, C. Maschler, and H. Ritsch, *Nat. Phys.* **3**, 319 (2007).
- [4] W. Chen, D. Meiser, and P. Meystre, *Phys. Rev. A* **75**, 023812 (2007).
- [5] N. Brahms, T. P. Purdy, D. W. C. Brooks, T. Botter, and D. M. Stamper-Kurn, *Nat. Phys.* **7**, 604 (2011).
- [6] P. Domokos and H. Ritsch, *Phys. Rev. Lett.* **89**, 253003 (2002).
- [7] D. Nagy, J. K. Asbóth, P. Domokos, and H. Ritsch, *Europhys. Lett.* **74**, 254 (2006).
- [8] D. Nagy, G. Szirmai, and P. Domokos, *Eur. Phys. J. D* **48**, 127 (2008).
- [9] A. T. Black, H. W. Chan, and V. Vuletić, *Phys. Rev. Lett.* **91**, 203001 (2003).
- [10] K. Baumann, C. Guerlin, F. Brennecke, and T. Esslinger, *Nature* **464**, 1301 (2010).
- [11] K. Baumann, R. Mottl, F. Brennecke, and T. Esslinger, *Phys. Rev. Lett.* **107**, 140402 (2011).
- [12] R. H. Dicke, *Phys. Rev.* **93**, 99 (1954).
- [13] K. Hepp and E. H. Lieb, *Ann. Phys.* **76**, 360 (1973).
- [14] Y. K. Wang and F. T. Hioe, *Phys. Rev. A* **7**, 831 (1973).
- [15] C. Emary and T. Brandes, *Phys. Rev. E* **67**, 066203 (2003).
- [16] F. Dimer, B. Estienne, A. S. Parkins, and H. J. Carmichael, *Phys. Rev. A* **75**, 013804 (2007).
- [17] D. Nagy, G. Konya, G. Szirmai, and P. Domokos, *Phys. Rev. Lett.* **104**, 130401 (2010).
- [18] F. Brennecke, R. Mottl, K. Baumann, R. Landig, T. Donner, and T. Esslinger, *Proc. Natl. Acad. Sci.* **110**, 11763 (2013).
- [19] E. G. Dalla Torre, S. Diehl, M. D. Lukin, S. Sachdev, and P. Strack, *Phys. Rev. A* **87**, 023831 (2013).
- [20] J. Larson, B. Damski, G. Morigi, and M. Lewenstein, *Phys. Rev. Lett.* **100**, 050401 (2008).
- [21] J. Larson, S. Fernández-Vidal, G. Morigi, and M. Lewenstein, *New J. Phys.* **10**, 045002 (2008).
- [22] D. M. Stamper-Kurn, “Cavity optomechanics with cold atoms,” [arXiv:1204.4351](https://arxiv.org/abs/1204.4351).
- [23] S. Gopalakrishnan, B. L. Lev, and P. M. Goldbart, *Nat. Phys.* **5**, 845 (2009).
- [24] S. Gopalakrishnan, B. L. Lev, and P. M. Goldbart, *Phys. Rev. A* **82**, 043612 (2010).
- [25] S. Gopalakrishnan, B. L. Lev, and P. M. Goldbart, *Phys. Rev. Lett.* **107**, 277201 (2011).
- [26] P. Strack and S. Sachdev, *Phys. Rev. Lett.* **107**, 277202 (2011).
- [27] M. Müller, P. Strack, and S. Sachdev, *Phys. Rev. A* **86**, 023604 (2012).
- [28] H. Ritsch, P. Domokos, F. Brennecke, and T. Esslinger, *Rev. Mod. Phys.* **85**, 553 (2013).
- [29] J. Larson, G. Morigi, and M. Lewenstein, *Phys. Rev. A* **78**, 023815 (2008).
- [30] R. Kanamoto and P. Meystre, *Phys. Rev. Lett.* **104**, 063601 (2010).
- [31] X. Guo, Z. Ren, G. Guo, and J. Peng, *Phys. Rev. A* **86**, 053605 (2012).
- [32] B. Padhi and S. Ghosh, *Phys. Rev. Lett.* **111**, 043603 (2013).
- [33] M. J. Bhaseen, J. Mayoh, B. D. Simons, and J. Keeling, *Phys. Rev. A* **85**, 013817 (2012).
- [34] The exactness of mean field theory in the  $N, \mathcal{A} \rightarrow \infty$  limit may be seen using a path-integral representation of  $f$ . After eliminating atomic fields, fluctuation corrections to the mean-field saddle point are suppressed by  $N/\mathcal{A}^2$ , and so vanish in the thermodynamic limit, as also occurs in the bosonic version of this model [41].
- [35] P. M. Chaikin and T. C. Lubensky, *Principles of Condensed Matter Physics* (Cambridge University Press, Cambridge, 1995).
- [36] A. I. Larkin and S. A. Pikin, *Sov. Phys. JETP* **29**, 891 (1969).
- [37] N. Liu, J. Lian, J. Ma, L. Xiao, G. Chen, J. Q. Liang, and S. Jia, *Phys. Rev. A* **83**, 033601 (2011).
- [38] E. T. Whittaker and G. N. Watson, *A Course of Modern Analysis* (Cambridge University Press, Cambridge, 1952).
- [39] J. Keeling, M. J. Bhaseen, and B. D. Simons, *Phys. Rev. Lett.* **105**, 043001 (2010).
- [40] S. H. Strogatz, *Nonlinear Dynamics and Chaos* (Perseus Books, Cambridge, Mass., 1994).
- [41] F. Piazza, P. Strack, and W. Zwerger, “Bose-Einstein Condensation versus Dicke-Hepp-Lieb Transition in an Optical Cavity,” [arXiv:1305.2928](https://arxiv.org/abs/1305.2928).